On the importance of vibrational contributions to small-angle optical rotation: Fluoro-oxirane in gas phase and solution

Cite as: J. Chem. Phys. **130**, 034310 (2009); https://doi.org/10.1063/1.3054301
Submitted: 10 October 2008 . Accepted: 02 December 2008 . Published Online: 21 January 2009

Thomas Bondo Pedersen, Jacob Kongsted, T. Daniel Crawford, and Kenneth Ruud

On the importance of vibrational contributions to small-angle optical rotation: Fluoro-oxirane in gas phase and solution

Thomas Bondo Pedersen,[1,a)] Jacob Kongsted,[1] T. Daniel Crawford,[2] and Kenneth Ruud[3]
[1]*Department of Theoretical Chemistry, Chemical Center, University of Lund, P.O. Box 124, S-221 00 Lund, Sweden*
[2]*Department of Chemistry, Virginia Tech, Blacksburg, Virginia 24061, USA*
[3]*Centre for Theoretical and Computational Chemistry (CTCC), Department of Chemistry, University of Tromsø, N-9037 Tromsø, Norway*

(Received 10 October 2008; accepted 2 December 2008; published online 21 January 2009)

The specific optical rotation of (S)-fluoro-oxirane in gas phase and solution is predicted using time-dependent density functional theory (B3LYP functional) and coupled cluster linear response theory. Upon vibrational averaging, the coupled cluster singles and doubles model predicts the gas phase specific optical rotation to be 8.1° $(\mathrm{dm\ g/cm^3})^{-1}$ at 355 nm at room temperature. This is an order of magnitude smaller than the B3LYP result of 68.4° $(\mathrm{dm\ g/cm^3})^{-1}$. The main source of this discrepancy is the electronic contribution at the equilibrium geometry. The effects of cyclohexane and acetonitrile solvents are calculated for both the electronic and vibrational contributions with the B3LYP functional. The specific optical rotation is estimated to change significantly depending on the polarity of the solvent, increasing in cyclohexane and decreasing in acetonitrile. © *2009 American Institute of Physics*. [DOI: 10.1063/1.3054301]

I. INTRODUCTION

Combined with experimental measurements, theoretical calculations of optical rotation may be used to determine the absolute configuration of chiral molecules, as recently demonstrated by Polavarapu,[1] Polavarapu and Chakraborty,[2,3] Beratan and co-workers,[4–6] and Stephens *et al.*[7–9] In principle, the task is simple: to distinguish enantiomers, calculate the specific optical rotation of a molecule using a first-principles method, and compare this to the experimentally observed specific rotation. If they agree, at least on the sign of the optical rotation, the absolute configuration is the one used in the theoretical calculation. In practice, the presence of multiple stereogenic centers complicates the assignment of absolute stereochemistry, and other chiroptical metrics must be included.[4–6] Needless to say, the first-principles methods must be reliable (in a statistical sense) for this approach to be successful. Stephens and co-workers,[9–11] using density functional theory (DFT), investigated the B3LYP exchange-correlation functional[12–14] and found that rather large basis sets including diffuse functions are required to obtain reasonable agreement between theory and experiment.

The vast majority of optical activity measurements is conducted in solution, whereas most theoretical calculations are performed for a single molecule in vacuum. Only recently, Vaccaro and co-workers[15,16] developed cavity ring-down polarimetry for the measurement of chiroptical properties in gas phase and thereby demonstrated that solvent effects may be dramatic, e.g., changing the sign of the rotation, and that they may even behave in nonintuitive ways. Solvent effects are, however, difficult to model, and the relatively simple and computationally tractable dielectric continuum models cannot always be trusted.[17,18] This was clearly demonstrated by Mukhopadhyay *et al.*[19,20] and Losada *et al.*,[21] who combined first-principles electronic optical rotation calculations with molecular dynamics and showed that explicit solvent molecules must be included to accurately describe the solvent effect on the optical rotation of methyloxirane.

The availability of accurate experimental optical rotations in gas phase may have been the spark that ignited the increasing interest in high-level *ab initio* methods for calculating gas phase optical activity over the past 7–8 years (see Refs. 22 and 23 for recent reviews of the field). An important result of recent research is that single-point calculations of the electronic optical activity are generally insufficient to give a complete account of experimental observations. For conformationally flexible molecules, Kondru *et al.*[24] and Wiberg *et al.*[25–29] showed that it is imperative to calculate the electronic optical activity for all conformations and to perform Boltzmann averaging over these. A number of studies have demonstrated that vibrational effects are non-negligible, including the work of Ruud *et al.*[30] and Mort and Autschbach.[31–34]

Most of the theoretical work outlined above is based on DFT, typically with the B3LYP exchange-correlation functional. A number of studies have appeared, which use the more advanced coupled cluster hierarchy of wave functions (see Refs. 22, 23, and 35 and references therein), often, but certainly not always, with substantial improvements in accuracy compared to DFT. We have recently studied the optical rotation of (S)-methyloxirane in gas phase using coupled cluster methods and demonstrated that a high-level electronic structure theory is necessary to obtain "the right answer for the right reason."[18,36–39] At first sight, it appears that coupled cluster models predict the wrong sign of the optical

a)Electronic mail: thomas.pedersen@teokem.lu.se.

TABLE I. Computed equilibrium geometries of (S)-fluoro-oxirane. Cartesian coordinates (Å) with the origin at the center of mass.

	B3LYP/aug-cc-pVTZ			CCSD(T)/cc-pVTZ		
Atom	*X*	*Y*	*Z*	*X*	*Y*	*Z*
O	0.829 651 4	−0.737 640 8	−0.160 220 7	0.826 186 5	−0.735 886 5	−0.159 183 8
C	−0.151 277 6	−0.000 395 9	0.478 147 1	−0.155 261 0	−0.002 037 7	0.475 553 1
C	0.986 825 2	0.708 280 1	−0.084 574 6	0.981 221 3	0.707 987 0	−0.083 859 0
F	−1.351 238 4	0.062 778 9	−0.169 891 4	−1.341 351 4	0.062 514 6	−0.169 540 6
H	−0.305 804 2	−0.181 377 6	1.535 827 5	−0.299 805 7	−0.176 297 7	1.529 808 7
H	0.852 318 2	1.221 355 7	−1.029 052 4	0.840 294 9	1.217 782 0	−1.023 952 2
H	1.796 816 4	1.050 350 7	0.548 861 8	1.785 726 7	1.049 036 6	0.549 092 7

rotation,[18,36–38] even when triple excitations are included in the coupled cluster wave function,[18] whereas B3LYP reproduces the experimental sign.[40] Adding zero-point vibrational effects calculated at the B3LYP level to the most accurate coupled cluster (CC3) results of Ref. 18, Ruud and Zanasi[41] showed that the correct sign is obtained, albeit with a slight overestimation compared to the experimental result of Müller *et al.*[15] Finally, Kongsted *et al.*[39] used coupled cluster theory to calculate both the electronic and the vibrational contributions to the specific optical rotation of (S)-methyloxirane and thus reproduced the experimental results to within a few degrees at three different wavelengths. Vibrational effects were also found to be crucial in the closely related case of (S)-methylthiirane, although the incorrect sign is obtained at short wavelengths.[23,42] The electronic contribution to the total optical rotation of (S)-methyloxirane is sensitive to the anharmonic torsional motion of the methyl group.[39] In order to eliminate this dependence, we here substitute the methyl group with a fluorine atom and thus predict the optical rotation of (S)-fluoro-oxirane.

While vibrational contributions are non-negligible for accurate optical activity predictions,[30–34] the sign of the optical rotation may often be determined with confidence without them. For molecules with small-angle optical rotations, however, vibrational effects must be taken into account, as the methyloxirane and methylthiirane cases clearly show. In addition, the effect of a potential solvent must be accounted for. However, the majority of previous studies of optical rotations consider either the effects of vibration *or* the effects of solvation. In fact, to the best of our knowledge, only one previous theoretical study have considered simultaneously the effects of solvation and molecular vibration.[43] The purpose of the present study is therefore twofold: (i) to predict the optical rotation of fluoro-oxirane in isolated form based on high-level coupled cluster calculations and (ii) to obtain further insights into the combined effects of vibration and solvation.

II. COMPUTATIONS

All calculations presented in this work have been carried out with development versions of the quantum chemistry programs PSI3 (Ref. 44) and DALTON.[45] We use the B3LYP exchange-correlation functional[12–14] for DFT calculations and second-order approximate coupled cluster singles and doubles (CC2),[46,47] full coupled cluster singles and doubles (CCSD),[48] and CCSD with perturbative triples corrections [CCSD(T)] (Ref. 49) for correlated wave function calculations. Dunning's[50] correlation-consistent basis sets augmented with diffuse functions are used throughout.

A. Gas phase equilibrium geometry

The effect of the nuclear geometry on electronic chiroptical properties can be significant, particularly for small-angle optical rotation. In this work, we optimize the geometry of (S)-fluoro-oxirane at the B3LYP and CCSD(T) levels of theory using the aug-cc-pVTZ and cc-pVTZ basis sets, respectively. Both the B3LYP and CCSD(T) optimizations are all-electron calculations. The optimized Cartesian coordinates reported in Table I reveal that the two calculated geometries are in overall close agreement. All B3LYP/aug-cc-pVTZ bond and dihedral angles agree with the CCSD(T)/cc-pVTZ ones to within 0.5°. The disagreement in the bond distances are on the order of milliangstrom, except for the C–F bond length, for which B3LYP/aug-cc-pVTZ and CCSD(T)/cc-pVTZ predict 1.365 and 1.352 Å, respectively.

B. Optical rotation in gas phase

The linear response approach[51] employed in this work does not take into account the finite lifetime of electronically excited states. As a consequence, the calculated dispersion curves become singular at the electronic excitation energies, and caution is required when applying this approach in the vicinity of the excitation energies. We therefore start by calculating the absorption and circular dichroism spectra of (S)-fluoro-oxirane in gas phase.

1. Electronic circular dichroism and optical rotation

Table II reports excitation energies, oscillator strengths, and rotatory strengths for the five lowest-lying electronic transitions (from the ground state). Oscillator and rotatory strengths are calculated and reported in length and velocity gauges, which are completely equivalent in exact theory but deviate in approximate models.[51–55] In a loose sense, the deviation between the length and velocity gauge results is a measure of the quality of the calculation: the more similar the length and velocity gauge results are, the better the calculation. Note, however, that gauge invariance is not a sufficient condition for a "converged" (with respect to correlation treatment as well as atomic orbital basis set) calculation.

TABLE II. Excitation energies (ΔE, nm), oscillator strength (f, dimensionless), and rotatory strength (R, 10^{-40} cgs) of the five lowest electronic transitions from the ground state of (S)-fluoro-oxirane. Oscillator and rotatory strengths are calculated in the LG, velocity gauge (VG), and employing GIAOs. All results are obtained with the aug-cc-pVTZ basis set, and the center of mass is used as a coordinate origin. (a) B3LYP/aug-cc-pVTZ and (b) CCSD(T)/cc-pVTZ equilibrium geometries.

	B3LYP					CC2					CCSD				
	1	2	3	4	5	1	2	3	4	5	1	2	3	4	5
(a)															
ΔE	167.6	161.0	158.4	156.3	151.1	163.9	158.7	154.0	147.9	146.0	151.2	150.1	141.9	140.2	137.1
f (LG)	0.015	0.009	0.010	0.007	0.020	0.015	0.014	0.013	0.009	0.029	0.010	0.016	0.009	0.017	0.047
f (VG)	0.015	0.009	0.010	0.007	0.021	0.014	0.013	0.012	0.008	0.029	0.011	0.017	0.009	0.017	0.044
R (LG)	15.61	−16.05	1.19	−2.40	−2.14	16.38	−12.27	0.00	−6.47	1.94	−14.86	18.80	2.18	−3.53	6.99
R (VG)	15.55	−16.09	1.21	−2.38	−1.82	15.89	−11.15	0.00	−6.67	2.52	−14.08	18.68	2.26	−3.92	6.54
R (GIAO)	15.56	−16.04	1.23	−2.42	−2.22										
(b)															
ΔE	167.9	160.9	158.6	156.9	151.5	163.9	158.6	153.9	148.4	146.3	151.0	150.2	141.9	140.6	137.5
f (LG)	0.014	0.009	0.009	0.008	0.020	0.015	0.014	0.013	0.009	0.030	0.009	0.017	0.007	0.019	0.046
f (VG)	0.014	0.009	0.009	0.008	0.020	0.014	0.013	0.012	0.009	0.028	0.009	0.017	0.007	0.019	0.044
R (LG)	15.36	−15.64	0.46	−2.12	−2.18	16.31	−12.20	−0.33	−6.24	1.70	−15.49	18.97	2.08	−3.62	7.85
R (VG)	15.31	−15.69	0.48	−2.10	−1.87	15.80	−11.07	−0.27	−6.42	2.25	−14.76	18.92	2.09	−3.93	7.39
R (GIAO)	15.31	−15.63	0.51	−2.15	−2.27										

For approximate models, the length gauge (LG) rotatory strength depends on the coordinate origin, chosen as the center of mass in our case, whereas the velocity gauge results are inherently origin invariant.[51,53–55] Rotatory strengths are also calculated and reported in the LG using gauge-including atomic orbitals (GIAOs) (also known as London orbitals). The GIAOs are mainly used to ensure origin invariance, a technique that only works for variational models such as DFT but fails for nonvariational ones like coupled cluster models.[51,53–55]

The changes in excitation energies due to differences in equilibrium geometry are in all cases less than approximately 0.5 nm. This is an order of magnitude smaller than the effect of improving the exchange-correlation treatment from the B3LYP density functional to the CC2 and CCSD wave function models. The at times rather large deviation between the B3LYP and the CC2/CCSD results is not too surprising, as the adiabatic time-dependent DFT employed in this work is a ground state theory. Note, in particular, that the CCSD model predicts the two lowest-lying (highest wavelength) transitions to be separated by less than 1 nm, while the CC2 and B3LYP models find the separation to be approximately 5 and 7 nm, respectively. Also for oscillator and rotatory strengths, the effect of the choice of equilibrium geometry is minute, whereas some variations are observed as a consequence of the exchange-correlation treatment. In particular, the B3LYP and CC2 models agree reasonably well for the two lowest-lying transitions, which are the most intense in the reported region of the circular dichroism spectrum. The CCSD model reverses the order of these two transitions, as revealed by the signs of the rotatory strengths, which are reversed for CCSD compared to CC2 and B3LYP. This can be viewed as an indication that a rather high level of electron correlation is required to accurately describe the optical properties of fluoro-oxirane.

Table III reports the electronic specific optical rotation calculated at 355 nm using the B3LYP, CC2, and CCSD models and the hierarchy of correlation-consistent basis sets augmented with diffuse functions. Results are given for both equilibrium geometries. As for rotatory strengths, the LG specific optical rotation is origin dependent, and we have chosen the center of mass as the coordinate origin. Although the velocity gauge is inherently origin invariant, it predicts an unphysical nonzero specific optical rotation at zero frequency (infinite wavelength) when used in conjunction with approximate models. The so-called modified velocity gauge[38] (MVG) corrects for this deficiency. In addition, B3LYP results calculated with GIAOs to ensure origin invariance are reported. From Table III we conclude that the basis set must be of at least triple-zeta quality for B3LYP as well as the coupled cluster models. However, Table III most clearly demonstrates the importance of correlation treatment: the B3LYP and coupled cluster models differ by as much as one order of magnitude. Discrepancies between B3LYP and coupled cluster optical rotations are caused by generally larger errors in the excitation energies and transition moments predicted by the former. This is particularly severe for small-angle optical rotation.

The dispersion curves in Fig. 1(a) show that the large difference between B3LYP and the coupled cluster models is present at all wavelengths (except at very large wavelengths where the specific optical rotation must be zero) and that it can be ascribed mainly to the underestimation of excitation energies by the B3LYP exchange-correlation functional. Another important feature of the dispersion curves of Fig. 1(a) is that the B3LYP specific optical rotation is strictly positive, whereas the coupled cluster curves change sign, indicating that not only excitation energies but also differing rotatory strengths give rise to the differences. While Table III reveals some dependence on the choice of equilibrium geometry, Fig. 1(a) shows that although the two equilibrium geometries are very similar, the effect on the calculated specific optical

TABLE III. (S)-fluoro-oxirane electronic specific optical rotation [deg (dm g/cm^3)$^{-1}$] at 355 nm. (a) B3LYP/aug-cc-pVTZ and (b) CCSD(T)/cc-pVTZ equilibrium geometry. Numbers in parentheses refer to the use of the corresponding doubly augmented basis set (*d*-aug-cc-pVXZ). The coordinate origin is chosen as the center of mass.

	$[\alpha]$						
	B3LYP			CC2		CCSD	
	LG	MVG	GIAO	LG	MVG	LG	MVG
(a)							
aug-cc-pVDZ	24.4	35.6	31.9	−31.4	−12.1	−24.8	−18.9
aug-cc-pVTZ	57.9	55.2	58.1	−11.9	2.5	−2.7(5.1)	0.5(8.4)
aug-cc-pVQZ	60.5	59.4	61.7	−8.3	6.0	2.7	6.8
aug-cc-pV5Z				−7.6	6.6		
(b)							
aug-cc-pVDZ	32.8	44.4	40.7	−21.4	−3.0	−16.3	−10.1
aug-cc-pVTZ	64.6	64.4	66.9	−1.4	11.9	−6.1	−9.8
aug-cc-pVQZ	69.4	68.4	70.6	2.3	15.7		
aug-cc-pV5Z				3.0	16.3		

rotation is relatively important. Of course, the relative effect is more significant for the coupled cluster models than for B3LYP, as the specific optical rotation is close to zero for the former. As can be seen in Fig. 1(b), however, the effect of equilibrium geometry is surprisingly similar for B3LYP and the coupled cluster models at all wavelengths.

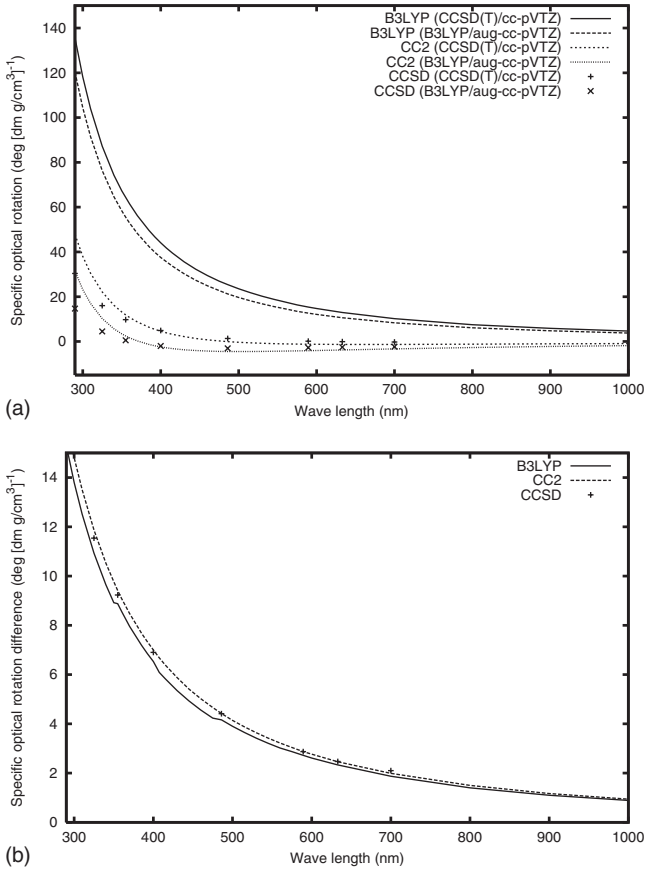

FIG. 1. Effect of geometry on the electronic specific optical rotation of (S)-F-oxirane: (a) electronic specific optical rotation dispersion computed with the MVG and the aug-cc-pVTZ basis set for the CCSD(T)/cc-pVTZ and B3LYP/aug-cc-pVTZ equilibrium geometries; (b) the difference between the CCSD(T)/cc-pVTZ and B3LYP/aug-cc-pVTZ geometries.

Figure 1(a) shows that the dispersion curves all turn upward as the wavelength decreases toward the first excitation energy. Based on the sign of the rotatory strengths of the lowest transition in Table II, one would indeed expect the B3LYP and CC2 curves to turn upward, but the CCSD curve should turn downward. To understand that the CCSD curve turns upward in Fig. 1(a), one needs to include contributions from both of the nearly degenerate lowest states. For all wavelengths above approximately 155 nm, the second CCSD state contributes by an amount larger than that of the first state (with opposite sign). For B3LYP and CC2, the first state gives rise to a larger contribution than the second state in the same spectral region. This sum-over-two-states analysis thus explains that the curves in Fig. 1(a) turn upward for all three methods. It must be stressed, however, that summing contributions from all five states reported in Table II cannot fully explain the features observed in Fig. 1(a).

2. Vibrational effects

A proper description of molecular response to external electromagnetic fields requires solving the complete Schrödinger equation, including electronic as well as nuclear degrees of freedom. Even within the Born–Oppenheimer approximation, this represents a formidable computational challenge. We here employ the computationally simpler approach of averaging over the vibrational modes in the electronic ground state. Following Refs. 56 and 57, as also done for methyloxirane in Ref. 39, the electronic specific optical rotation is considered a function of the vibrational degrees of freedom (normal coordinates) and Taylor expanded to second order about a reference geometry. Two types of reference geometries are considered: the equilibrium geometry corresponds to averaging in the harmonic approximation, whereas the so-called effective geometry includes anharmonic effects in addition to harmonic contributions. We estimate the temperature dependence of the specific optical rotation using the same formulas as in Ref. 39. Without further justification, we

TABLE IV. Electronic and harmonic vibrational contributions to the specific optical rotation [deg $(\mathrm{dm\ g/cm^3})^{-1}$] calculated with the aug-cc-pVTZ basis set. The results are based on the equilibrium B3LYP/aug-cc-pVTZ geometry of (S)-fluoro-oxirane, and the harmonic vibrational contribution is reported at two temperatures. The coordinate origin is chosen as the center of mass. Wavelength (λ) is given in nm. (a) LG; (b) MVG.

			$[\alpha]^{\mathrm{har}}_{\mathrm{eq}}$		$\langle[\alpha]\rangle$	
Model	λ	$[\alpha]^{\mathrm{el}}_{\mathrm{eq}}$	0 K	298.15 K	0 K	298.15 K
(a)						
B3LYP	355	57.89	12.95	12.76	70.84	70.65
	589.3	13.82	3.51	3.44	17.33	17.26
	633	11.61	2.98	2.93	14.59	14.53
CCSD	355	−2.72	6.63	6.42	3.91	3.70
	589.3	−3.32	2.00	1.94	−1.32	−1.38
	633	−3.00	1.63	1.57	−1.37	−1.43
(b)						
B3LYP	355	55.20	14.56	14.40	69.76	69.60
	589.3	12.68	4.06	4.00	16.74	16.68
	633	10.61	3.45	3.41	14.06	14.02
CCSD	355	0.53	8.55	8.22	9.08	8.75
	589.3	−2.77	2.76	2.66	−0.01	−0.11
	633	−2.56	2.39	2.31	−0.17	−0.25

thus calculate the temperature dependence of the harmonic contribution while keeping the anharmonic contribution constant at its zero-point value.

Table IV reports vibrationally averaged specific optical rotations obtained using the B3LYP/aug-cc-pVTZ equilibrium structure as reference geometry. Consequently, only harmonic vibrational effects are included. The rigidity of fluoro-oxirane, i.e., the absence of low-frequency modes such as torsion, makes the specific optical rotation nearly independent of temperature, at least up to room temperature. On this point B3LYP and CCSD agree, although there is some discrepancy between the harmonic vibrational contributions predicted by the two methods. This discrepancy is, however, an order of magnitude smaller than the difference between the electronic contributions calculated at the B3LYP and CCSD levels of theory. The same can be observed for the anharmonic contributions listed in Table V where the B3LYP/aug-cc-pVTZ effective geometry is used as reference geometry. Comparing the total specific optical rotations in Tables IV and V, it is evident that anharmonicity is insignificant for this molecule.

The large difference between the vibrationally averaged B3LYP and CCSD results thus stems from the discrepancy between the electronic contributions at the equilibrium ge-

TABLE V. Electronic, harmonic, and anharmonic vibrational contributions to the specific optical rotation [deg $(\mathrm{dm\ g/cm^3})^{-1}$] calculated with the aug-cc-pVTZ basis set. The results are based on the equilibrium and effective B3LYP/aug-cc-pVTZ geometries of (S)-fluoro-oxirane, and the harmonic vibrational contribution is reported at two temperatures. The coordinate origin is chosen as the center of mass. Wavelength (λ) is given in nm. (a) LG; (b) MVG.

				$[\alpha]^{\mathrm{har}}_{\mathrm{eff}}$		$\langle[\alpha]\rangle$	
Model	λ	$[\alpha]^{\mathrm{el}}_{\mathrm{eq}}$	$[\alpha]^{\mathrm{anh}}$	0 K	298.15 K	0 K	298.15 K
(a)							
B3LYP	355	57.89	−1.22	13.13	12.89	69.80	69.56
	589.3	13.82	−0.36	3.56	3.48	17.02	16.94
	633	11.61	−0.30	3.03	2.96	14.34	14.27
CCSD	355	−2.72	−2.55	8.11	7.87	2.84	2.60
	589.3	−3.32	−0.79	2.35	2.28	−1.76	−1.83
	633	−3.00	−0.68	2.00	1.94	−1.68	−1.74
(b)							
B3LYP	355	55.20	−1.17	14.59	14.37	68.62	68.40
	589.3	12.68	−0.34	4.07	4.00	16.41	16.34
	633	10.61	−0.29	3.47	3.41	13.79	13.73
CCSD	355	0.53	−2.01	9.93	9.58	8.45	8.10
	589.3	−2.77	−0.65	2.81	2.71	−0.61	−0.71
	633	−2.56	−0.56	2.40	2.30	−0.72	−0.82

TABLE VI. Solvent effects ($\Delta P = P_{solv} - P_{vac}$) on the electronic, harmonic, and anharmonic vibrational contributions to the specific optical rotation [deg $(\mathrm{dm\ g/cm^3})^{-1}$]. The results are calculated at the B3LYP/aug-cc-pVTZ level using the LG and are based on the equilibrium B3LYP/aug-cc-pVTZ geometry and effective B3LYP/aug-cc-pVTZ geometries of (S)-fluoro-oxirane. The coordinate origin is chosen as the center of mass. The unit of wavelength (λ) is nm, and the temperature is 0 K.

Solvent	λ	$\Delta[\alpha]^{el}_{eq}$	$\Delta[\alpha]^{har}_{eff}$	$\Delta[\alpha]^{anh}$	$\Delta\langle[\alpha]\rangle$
Cyclohexane	355	−2.15	20.68	2.53	21.06
	589.3	0.07	16.03	0.75	16.85
	633	0.10	14.27	0.63	15.00
Acetonitrile	355	−20.04	−29.79	5.86	−43.97
	589.3	−4.28	−6.40	1.85	−8.82
	633	−3.57	−5.34	1.59	−7.33

ometry. This observation shows that it might be possible to calculate vibrational contributions at the B3LYP level and add these to the electronic contribution calculated at the CCSD level of theory and still get an accurate prediction of the total (vibrationally averaged) specific optical rotation. In terms of computer time, such an approach would be significantly less demanding than performing a complete CCSD simulation.

C. Solvent effects

While specific optical rotation of organic molecules is most often measured in solution, theoretical studies are dominated by gas phase (i.e., single molecule) computations, which are far less expensive and much simpler to perform than calculations of solvent effects. To simulate solvation, we use the polarizable continuum model and calculate the solvent effect on electronic as well as vibrational contributions to the specific optical rotation at the B3LYP level. For details about the theoretical method, see Refs. 17, 58, and 59. Using a nonequilibrium solvation scheme, the cavity is built by interlocking spheres centered on functional groups (united atom approach). The radii used are 2.04 Å for CH, 2.28 Å for CH_2, and 1.5 Å for O and F.[60] A scaling factor of 1.2 is used for enlarging the cavity.

The solvent effects, defined as the difference between the solution phase and the gas phase, on the electronic and vibrational contributions to the specific optical rotation of (S)-fluoro-oxirane in a nonpolar (cyclohexane) and a polar (acetonitrile) solvent are given in Table VI. For both cyclohexane and acetonitrile, the solvent effect on the total specific optical rotation is of the same order of magnitude as the gas phase value itself, and the sign of the effect depends on the polarity of the solvent. The total specific optical rotation increases in cyclohexane and decreases in acetonitrile. The absolute value of the solvent effects decreases with increasing wavelength, as it must (the total rotation must vanish in the static limit). The solvent effect is almost completely accounted for by the harmonic vibrational contribution in cyclohexane, whereas both the electronic and harmonic contributions decrease significantly in acetonitrile.

III. CONCLUDING REMARKS

Based on the (S)-methyloxirane case,[39] it may be assumed that the CCSD model (using the MVG) provides the most accurate estimate for the gas phase optical rotation of (S)-fluoro-oxirane at 355 nm: +8.45° $(\mathrm{dm\ g/cm^3})^{-1}$ at 0 K, slightly decreasing to +8.10° $(\mathrm{dm\ g/cm^3})^{-1}$ at 298.15 K. Vibrational effects account for approximately 94% of these values. At 589.3 and 633 nm, vibrational effects are smaller and effectively annihilate the chiroptical response in the gas phase. Solvent effects, calculated at the B3LYP level of theory, significantly change the vibrational contributions by approximately +23° $(\mathrm{dm\ g/cm^3})^{-1}$ in cyclohexane and by −24° $(\mathrm{dm\ g/cm^3})^{-1}$ in acetonitrile at 355 nm. We thus find that both vibrational and solvent effects are crucial for an accurate description of small-angle specific optical rotation.

To improve the accuracy of the results of the present work, one would have to

(1) improve the electron correlation description,
(2) include the temperature dependence of the anharmonic vibrational contribution, and
(3) take into account the induced chiral configuration of solvent molecules.

The obvious, if computationally expensive, choice for point 1 would be to include triple excitations in the coupled cluster wave function and calculate the electronic specific optical rotation at the reference geometry, as done for methyloxirane in Ref. 18. A proper account of temperature dependence, point 2, is obtained by calculating the effective geometry at each temperature. Finally, point 3 requires inclusion of explicit solvent molecules in the quantum mechanical calculation, as done for methyloxirane in Refs. 19–21.

ACKNOWLEDGMENTS

This work has been supported by the Swedish Foundation for Strategic Research. J.K. acknowledges support from the Villum Kann Rasmussen Foundation (Denmark). T.D.C. was supported by a grant from the National Science Foundation (Grant No. CHE-0715185) and a subcontract from Oak Ridge National Laboratory by the Scientific Discovery through the Advanced Computing (SciDAC) program of the Division of Basic Energy Science, Office of Science, U.S.

Department of Energy under Contract No. DE-AC05-00OR22725 with Oak Ridge National Laboratory. K.R. has received support from the Norwegian Research Council through a Centre of Excellence grant (Grant No. 179568/V30) and a YFF grant (Grant No. 162746/V00).

[1] P. L. Polavarapu, Mol. Phys. **91**, 551 (1997).
[2] P. L. Polavarapu and D. K. Chakraborty, J. Am. Chem. Soc. **120**, 6160 (1998).
[3] P. L. Polavarapu and D. K. Chakraborty, Chem. Phys. **240**, 1 (1999).
[4] R. K. Kondru, P. Wipf, and D. N. Beratan, J. Am. Chem. Soc. **120**, 2204 (1998).
[5] S. Ribe, R. K. Kondru, D. N. Beratan, and P. Wipf, J. Am. Chem. Soc. **122**, 4608 (2000).
[6] M. Goldsmith, N. Jayasuriya, D. N. Beratan, and P. Wipf, J. Am. Chem. Soc. **125**, 15696 (2003).
[7] P. J. Stephens, F. J. Devlin, J. R. Cheeseman, M. J. Frisch, and C. Rosini, Org. Lett. **4**, 4595 (2002).
[8] P. J. Stephens, D. M. McCann, F. J. Devlin, J. R. Cheeseman, and M. J. Frisch, J. Am. Chem. Soc. **126**, 7514 (2004).
[9] P. J. Stephens, D. M. McCann, J. R. Cheeseman, and M. J. Frisch, Chirality **17**, S52 (2005).
[10] J. R. Cheeseman, M. J. Frisch, F. J. Devlin, and P. J. Stephens, J. Phys. Chem. A **104**, 1039 (2000).
[11] P. J. Stephens, F. J. Devlin, J. R. Cheeseman, and M. J. Frisch, J. Phys. Chem. A **105**, 5356 (2001).
[12] A. D. Becke, J. Chem. Phys. **98**, 5648 (1993).
[13] C. Lee, W. Yang, and R. G. Parr, Phys. Rev. B **37**, 785 (1988).
[14] B. Miehlich, A. Savin, H. Stoll, and H. Preuss, Chem. Phys. Lett. **157**, 200 (1989).
[15] T. Müller, K. B. Wiberg, and P. H. Vaccaro, J. Phys. Chem. A **104**, 5959 (2000).
[16] T. Müller, K. B. Wiberg, P. H. Vaccaro, J. R. Cheeseman, and M. J. Frisch, J. Opt. Soc. Am. B **19**, 125 (2002).
[17] B. Mennucci, J. Tomasi, J. R. Cheeseman, M. J. Frisch, F. J. Devlin, S. Gabriel, and P. J. Stephens, J. Phys. Chem. A **106**, 6102 (2002).
[18] J. Kongsted, T. B. Pedersen, M. Strange, A. Osted, Aa. E. Hansen, K. V. Mikkelsen, F. Pawlowski, P. Jørgensen, and C. Hättig, Chem. Phys. Lett. **401**, 385 (2005).
[19] P. Mukhopadhyay, G. Zuber, M. Goldsmith, P. Wipf, and D. N. Beratan, ChemPhysChem **7**, 2483 (2006).
[20] P. Mukhopadhyay, G. Zuber, P. Wipf, and D. N. Beratan, Angew. Chem., Int. Ed. **46**, 6450 (2007).
[21] M. Losada, P. Nguyen, and Y. Xu, J. Phys. Chem. A **112**, 5621 (2008).
[22] T. D. Crawford, Theor. Chem. Acc. **115**, 227 (2006).
[23] T. D. Crawford, M. C. Tam, and M. L. Abrams, J. Phys. Chem. A **111**, 12057 (2007).
[24] R. K. Kondru, P. Wipf, and D. N. Beratan, J. Phys. Chem. A **103**, 6603 (1999).
[25] K. B. Wiberg, P. H. Vaccaro, and J. R. Cheeseman, J. Am. Chem. Soc. **125**, 1888 (2003).
[26] K. B. Wiberg, Y. Wang, P. H. Vaccaro, J. R. Cheeseman, G. Trucks, and M. J. Frisch, J. Phys. Chem. A **108**, 32 (2004).
[27] K. B. Wiberg, Y. Wang, P. H. Vaccaro, J. R. Cheeseman, and M. R. Luderer, J. Phys. Chem. A **109**, 3405 (2005).
[28] K. B. Wiberg, S. M. Wilson, P. H. Vaccaro, and J. R. Cheeseman, J. Phys. Chem. A **109**, 3448 (2005).
[29] K. B. Wiberg, Y. Wang, S. M. Wilson, P. H. Vaccaro, W. L. Jorgensen, T. D. Crawford, M. L. Abrams, J. R. Cheeseman, and M. Luderer, J. Phys. Chem. A **112**, 2415 (2008).
[30] K. Ruud, P. R. Taylor, and P.-O. Åstrand, Chem. Phys. Lett. **337**, 217 (2001).
[31] B. C. Mort and J. Autschbach, J. Phys. Chem. A **109**, 8617 (2005).
[32] B. C. Mort and J. Autschbach, J. Phys. Chem. A **110**, 11381 (2006).
[33] B. C. Mort and J. Autschbach, ChemPhysChem **8**, 605 (2007).
[34] B. C. Mort and J. Autschbach, ChemPhysChem **9**, 159 (2008).
[35] T. D. Crawford and P. J. Stephens, J. Phys. Chem. A **112**, 1339 (2008).
[36] K. Ruud, P. J. Stephens, F. J. Devlin, P. R. Taylor, J. R. Cheeseman, and M. J. Frisch, Chem. Phys. Lett. **373**, 606 (2003).
[37] M. C. Tam, N. J. Russ, and T. D. Crawford, J. Chem. Phys. **121**, 3550 (2004).
[38] T. B. Pedersen, H. Koch, L. Boman, and A. M. J. Sánchez de Merás, Chem. Phys. Lett. **393**, 319 (2004).
[39] J. Kongsted, T. B. Pedersen, L. Jensen, Aa. E. Hansen, and K. V. Mikkelsen, J. Am. Chem. Soc. **128**, 976 (2006).
[40] E. Giorgio, C. Rosini, R. G. Viglione, and R. Zanasi, Chem. Phys. Lett. **376**, 452 (2003).
[41] K. Ruud and R. Zanasi, Angew. Chem., Int. Ed. Engl. **44**, 3594 (2005).
[42] T. D. Crawford, M. C. Tam, and M. L. Abrams, Mol. Phys. **105**, 2607 (2007).
[43] J. Kongsted and K. Ruud, Chem. Phys. Lett. **451**, 226 (2008).
[44] T. D. Crawford, C. D. Sherrill, E. F. Valeev, J. T. Fermann, R. A. King, M. L. Leininger, S. T. Brown, C. L. Janssen, E. T. Seidl, J. P. Kenny, and W. D. Allen, J. Comput. Chem. **28**, 1610 (2007).
[45] DALTON, Release 2.0, a molecular electronic structure program, 2005 (see http://www.kjemi.uio.no/software/dalton.html).
[46] O. Christiansen, H. Koch, and P. Jørgensen, Chem. Phys. Lett. **243**, 409 (1995).
[47] T. B. Pedersen, A. M. J. Sánchez de Merás, and H. Koch, J. Chem. Phys. **120**, 8887 (2004).
[48] G. D. Purvis and R. J. Bartlett, J. Chem. Phys. **76**, 1910 (1982).
[49] K. Raghavachari, G. W. Trucks, J. A. Pople, and M. Head-Gordon, Chem. Phys. Lett. **157**, 479 (1989).
[50] T. H. Dunning, Jr., J. Chem. Phys. **90**, 1007 (1989).
[51] T. B. Pedersen and H. Koch, J. Chem. Phys. **106**, 8059 (1997).
[52] T. B. Pedersen and H. Koch, Chem. Phys. Lett. **293**, 251 (1998).
[53] T. B. Pedersen, H. Koch, and K. Ruud, J. Chem. Phys. **110**, 2883 (1999).
[54] T. B. Pedersen, H. Koch, and C. Hättig, J. Chem. Phys. **110**, 8318 (1999).
[55] T. B. Pedersen, B. Fernández, and H. Koch, J. Chem. Phys. **114**, 6983 (2001).
[56] P.-O. Åstrand, K. Ruud, and P. R. Taylor, J. Chem. Phys. **112**, 2655 (2000).
[57] K. Ruud, P.-O. Åstrand, and P. R. Taylor, J. Chem. Phys. **112**, 2668 (2000).
[58] J. Tomasi, B. Mennucci, and R. Cammi, Chem. Rev. (Washington, D.C.) **105**, 2999 (2005).
[59] M. Pecul, D. Marchesan, K. Ruud, and S. Coriani, J. Chem. Phys. **122**, 024106 (2005).
[60] V. Barone, M. Cossi, and J. Tomasi, J. Chem. Phys. **107**, 3210 (1997).